RSC Advances

PAPER

View Article Online
View Journal | View Issue

Cite this: *RSC Adv.*, 2020, **10**, 44103

Developing non-isocyanate urethane-methacrylate photo-monomers for 3D printing application†

Neelima Singh, Hadi Bakhshi * and Wolfdietrich Meyer

Urethane-methacrylate photo-monomers were prepared *via* a non-isocyanate route for the 3D printing application. The monomers were synthesized through reacting aliphatic amines, *i.e.* 1,6-hexanediamine, 1,4-butanediol bis(3-aminopropyl) ether, or *n*-butylamine, with cyclic carbonates, *i.e.* ethylene carbonate or propylene carbonate, followed by the methacrylation of the generated hydroxylurethanes. The effects of the chemical structure of monomers on their photo-reactivity and physicomechanical properties of the cured samples were studied. Propylene carbonate generated side methyl groups within the urethane block, which significantly limited the crystallization of the monomers resulting in high photo-reactivity ($R_{p,max}$ = 6.59 × 10^{-2} s^{-1}) and conversion (DBC_{total} = 85%). The ether bonds of 1,4-butanediol bis(3-aminopropyl) ether decreased the intermolecular hydrogen bonding between urethane blocks, which not only improved the photo-reactivity ($R_{p,max}$ = 8.18 × 10^{-2} s^{-1}) and conversion (DBC_{total} = 86%) of the monomer but led to a high crosslinking density (ν_c = 5140 mol m^{-3}) and more flexibility for the cured sample. An ink was developed based on the monomers and successfully 3D printed on a digital light processing machine. In the absence of toxic isocyanates and tin compounds, the non-isocyanate route can be employed to develop urethane-methacrylates with desirable photo-reactivity and physicomechanical properties as good candidates to formulate inks for 3D printing of biomedical materials.

Received 22nd July 2020
Accepted 2nd December 2020

DOI: 10.1039/d0ra06388f

rsc.li/rsc-advances

Introduction

Urethane-methacrylates are interesting photo-monomers to generate networks with high mechanical stability. These monomers are used in the formulation of UV-curable coatings[1] and adhesives,[2] dental restorative materials,[3] and stereolithography.[4,5] The intermolecular hydrogen bonding between the urethane blocks of monomers grants the pre-association of molecules and thus 3–6 times faster photo-curing compared to their corresponding non-hydrogen bonding methacrylates.[6–8] Furthermore, the hydrogen bonding causes the superior mechanical strength for the cured samples.[9,10] Therefore, urethane-methacrylates are ideal candidates for developing fast-curable formulations, where high mechanical properties such as tensile and flexural strengths for the final material are expected.

Urethane-methacrylates are usually synthesized from the reaction of polyisocyanates and hydroxyalkyl methacrylates.[10–12] The principal limitation of this route is the high toxicity of isocyanates to the environment and humans.[13–15] Isocyanates are one of the frequently reported sources for chemical-induced occupational asthma[16] since they can react with hydroxyl, amine, and carboxylic acid functions of the human body's proteins in terms of inhalation or skin/eye contact.[13–15] Although it is assumed that isocyanates are completely converting during the synthesis, traces of unreacted isocyanate residues were detected in the final polyurethane materials,[17,18] which are toxic for the users.[19,20] Tin-based catalysts, *e.g.* dibutyl-tin-dilaurate (DBTDL), which is not removed after the reaction led to the toxicity for urethane-methacrylates even after photo-curing.[21,22] Therefore, synthesis of urethane-methacrylates excluding isocyanates and tin-based catalysts is valuable, especially for the fabrication of biomedical, food packaging, and children products.

One non-isocyanate route to synthesize urethane-methacrylates is through the ring-opening reaction of cyclic carbonates with primary amines, which generates hydroxylurethanes.[7,23–26] In contrast to isocyanates, cyclic carbonates are not toxic or moisture-sensitive to require special safety care during storage and handling.[27] The pendant hydroxyl groups allow further functionalization reactions, *e.g.* methacrylation.[7,23,24,28,29] On this subject, Wang *et al.*[28] synthesized urethane-methylates through the mentioned non-isocyanate route as reactive diluents for UV-curable polyurethane coatings. Meng *et al.*[23,24] prepared also urethane-methylates *via* the same route for emulsion polymerization.

Recently, photo-curing 3D printing technology is vastly utilizing for medical applications.[30,31] It can be used to rapidly manufacture personalized implants and organs, which perfectly

Department of Functional Polymer Systems, Fraunhofer Institute for Applied Polymer Research IAP, Geiselbergstraße 69, 14476 Potsdam, Germany. E-mail: hadi.bakhshi@iap.fraunhofer.de; Tel: +49-331-568-1425

† Electronic supplementary information (ESI) available: Experimental details and extra results. See DOI: 10.1039/d0ra06388f

match the patient's damaged tissue.[31] The suitable mechanical strength, bioactivity, biodegradability/biostability, and particularly biocompatibility of the employed materials are effective for the proper function of the 3D printed implant in the body and tissue repairing process. Regarding biocompatibility, the majority of photo-curable inks are cytotoxic, due to the unreacted monomers, photoinitiator resides, and toxic impurities. Therefore, developing photo-curable 3D printing inks for direct and long-term implantation in the body is still in research. As mentioned before, the synthesis of urethane-methacrylates through a non-isocyanate route is valuable for developing a biocompatible photo-curable ink. On this subject, Warner *et al.*[32] synthesized a non-isocyanate urethane-ally compound to develop thiol–ene inks for digital light processing (DLP) printing, which did not expose any toxic effect against murine myoblasts.

In this work, we prepared urethane-methacrylate photo-monomers to develop 3D printable inks employing non-isocyanate urethane chemistry without using toxic isocyanates and tin compounds. For this purpose, different aliphatic primary diamines or amine, *i.e.* 1,6-hexanediamine (1,6-HDA), 1,4-butanediol bis(3-aminopropyl)ether (1,4-BBE), or *n*-butylamine (*n*-BA), were reacted with cyclic carbonates, *i.e.* ethylene carbonate (EC) or propylene carbonate (PC), to generate hydroxylurethanes. Later, the hydroxyl groups of hydroxylurethanes reacted with methacrylate anhydride (MAAn) to synthesize urethane-methacrylates. The effects of the chemical structure of monomers on their photo-reactivity and physicomechanical properties of the cured samples were studied. The 3D printability of a formulation based on the monomers was tested on a DLP printer.

Experimental

All experimental details including materials, synthesis procedures, instruments, methods are provided in the ESI.†

Results and discussion

Synthesis of urethane-methacrylates

Non-isocyanate urethane chemistry was employed to develop urethane-methacrylate photo-monomers in two steps. In the first step, aliphatic primary diamines (1,6-HDA or 1,4-BBE) or amine (*n*-BA) were reacted with cyclic carbonates (EC or PC) without using any catalyst to generate hydroxylurethanes (Fig. 1).[7,23,24,28,33] FTIR spectra obtained from the reaction mixtures showed the disappearance of the peak at 1795 cm^{-1} corresponding to the carbonyl (C=O) bond of the cyclic carbonate moiety and the appearance of three new peaks at 1525, 1710, and 3320 cm^{-1} attributing to the generated urethane and hydroxyl groups (Fig. S1 in ESI†).[34,35] The aminolysis of EC with the primary amines was fast without using any catalyst. For example, the reaction of EC with 1,6-HDA was completed within 1 h at 25 °C. However, the reaction of PC with 1,6-HDA was very slow requiring a high reaction time (48 h) and temperature (60 °C, Fig. S1 in ESI†). The low reactivity of PC against the primary amines has been previously reported.[36] The presence of the electron-releasing methyl group within PC decreases the partial polarity of the carbonyl bond and consequently reduces its reactivity for the nucleophilic reactions.[37,38]

The methyl group of PC can result in constitutional isomerization during the ring–opening reaction. Therefore, the reaction of PC and 1,6-HAD led to three products; one with two primary hydroxyl groups, one with two secondary hydroxyl groups, and one with a primary and a secondary hydroxyl groups (synthesis of UrDMA2 in ESI†). According to the ^{1}H-NMR integration values (Fig. S2 in ESI†), the ring–opening reaction of PC from γ-position of the methyl group (59%) resulting in the primary hydroxyl group was more possible than the β-position (41%) leading to the secondary hydroxyl group, which was in agreement with previous reports.[36,39] It can be attributed to the steric hindrance effect of the methyl moiety during the attack of nucleophiles (primary amine groups). Increasing the reaction temperature from 25 °C to 60 °C did not change the ratio of primary to secondary hydroxyl groups within the final product (Urdiol2). In the case of EC, only one hydroxylurethane, with the primary hydroxyl groups was obtained (synthesis of UrDMA1, UrDMA3, and UrMA1 in ESI†). The chemical structure of all synthesized hydroxylurethanes was studied by FTIR and NMR spectroscopies. The results were in agreement with their expected molecular structures (Fig. S2 and S3 in ESI†). According to the ^{1}H-NMR integration values, the yield of the aminolysis reaction was 100% for all synthesized hydroxylurethanes.

In the second step, the hydroxyl groups of hydroxylurethanes were reacted with MAAn using DMAP as a catalyst and TEA as an acid scavenger at room temperature (Fig. 1).[7,23,24,28] Due to the

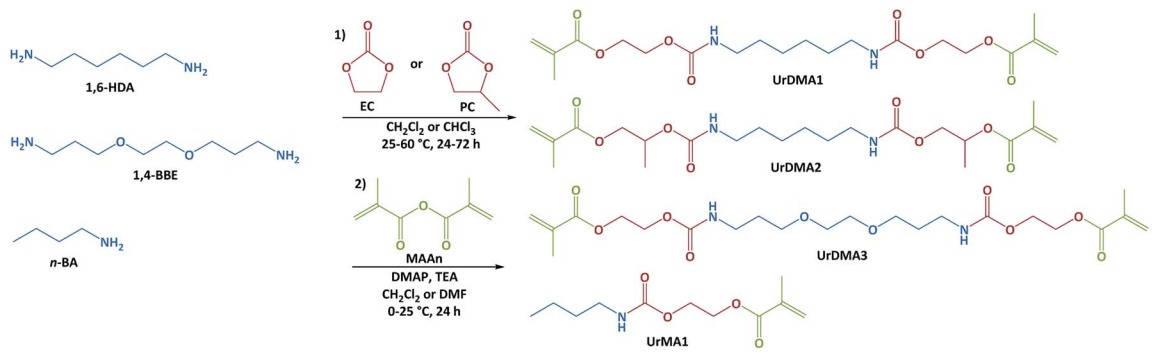

Fig. 1 Two-step non-isocyanate route for the synthesis of urethane-methacrylate monomers.

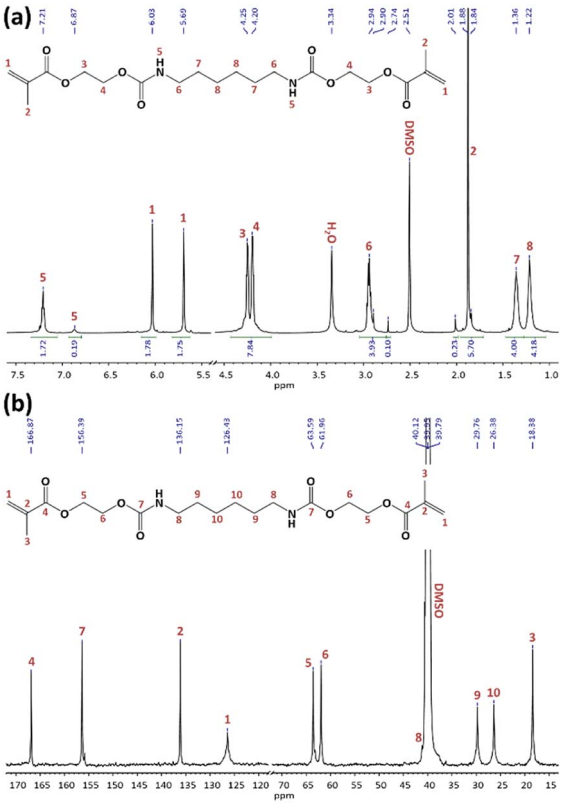

Fig. 2 ^{1}H-NMR (a) and ^{13}C-NMR (b) spectra for UrDMA1 in DMSO-d_6.

exothermic nature of the methacrylation reaction, the hydroxylurethane solutions were initially cooled down to 0 °C. The chemical structure of all synthesized monomers was studied by FTIR and NMR spectroscopies (ESI†). FTIR spectra confirmed the successful methacrylation, while the sharpness of the peak at 3320 cm^{-1} relating to the hydroxyl groups of hydroxylurethanes was decreased and a shoulder peak at 1640 cm^{-1} regarding the double bonds (C=C) of methacrylate moieties appeared. The NMR spectra for UrDMA1 are presented in Fig. 2. All peaks are assigned with the corresponding protons or carbons in the embedded molecular structure of UrDMA1. The urethane protons yielded two signals at 6.87 and 7.21 ppm regarding the pseudo *E* and *Z* conformations.[33,40] The protons of the methacrylate moieties appeared at 1.88, 5.69, and 6.03 ppm.[7] Meanwhile, the carbons of carbonyl bonds within the urethane and methacrylate moieties led to signals at 156.39 and 166.87 ppm.[7,33,40] According to the ^{1}H-NMR integration values, the yield of the methacrylation reaction was 100% for all synthesized monomers.

The physical state of the photo-monomers is important for the ease of formulating photo-curable inks. Therefore, the melting points (T_m) of the monomers were evaluated by DSC (Table 1 and Fig. S4 in ESI†). Due to the thermal-sensitivity of the monomers, the first heating cycle was used for the extraction of T_m values (peak maximum). UrDMA1 was a white powder with a T_m of 76 °C, thus it needs to be melted or dissolved in a reactive dilute before photo-curing. The T_m of UrDMA1 was depended on its purity. Thus, the T_m of UrDMA1 synthesized here with high purity was 20 °C higher than the reported value (56–57 °C (ref. 7)). UrDMA2 was a colorless low-viscose liquid that did not show any T_m by cooling, while it underwent a glass transition (T_g) at −57 °C (Fig. S4 in ESI†). The UrDMA2 molecules as a mixture of three constitutional isomers were sterically hindered by two methyl groups to form intermolecular hydrogen bonding, pack in and make a crystalline domain.[7] UrDMA3 was a waxy solid with a T_m of 31 °C. The lower T_m and crystallinity (ΔH_m = 5.0 J g^{-1}) of UrDMA3 comparing to UrDMA1 (ΔH_m = 109.9 J g^{-1}) is attributed to the presence of two ether bonds within its molecular structure, which can make hydrogen bonds with the urethane moieties and consequently increases the ratio of intramolecular to intermolecular hydrogen bonding. Monofunctional UrMA1 was a colorless liquid with a T_m of 3 °C. Due to low viscosity (35 mPa s), it can be used as a reactive diluent for other difunctional urethane-methacrylates.

T_p: temperature of photo-curing, $R_{p,max}$: maximum photo-curing rate, t_{max}: time to reach $R_{p,max}$, $\Delta H_{p,total}$: total generated photo-curing heat, DBC_{total}: total double bond conversion, $t_{95\%}$: time to reach 95% of DBC_{total}.

Photo-reactivity of urethane-methacrylates

The photo-reactivity of the monomers was studied using photo-DSC in isothermal mode. Each monomer was mixed with ethyl phenyl(2,4,6-trimethylbenzoyl)phosphinate (TPO-L, 3 wt%) as a photoinitiator before analysis at 25 °C with a UV intensity of 1 W m^{-2}. UrDMA1 was warmed up to melt before mixing with

Table 1 Thermal properties and photo-reactivity of urethane-methacrylates[a]

	DSC		Photo-DSC					
Monomer	T_m (°C)	ΔH_m (J g^{-1})	T_p (°C)	$R_{p,max}$ (s^{-1})	t_{max} (s)	$\Delta H_{p,total}$ (J g^{-1})	DBC_{total} (%)	$t_{95\%}$ (s)
UrDMA1	76	109.9	25	4.72×10^{-3}	61.4	5.8	2	99.3
			80	2.68×10^{-2}	13.3	121.2	47	49.6
UrDMA2	—	—	25	6.59×10^{-2}	13.4	254.8	85	33.6
UrDMA3	31	5.0	25	8.18×10^{-2}	10.9	182.9	86	29.1
UrMA1	3	34.1	25	6.61×10^{-2}	19.5	247.5	98	32.9

[a] T_p: temperature of photo-curing, $R_{p,max}$: maximum photo-curing rate, t_{max}: time to reach $R_{p,max}$, $\Delta H_{p,total}$: total generated photo-curing heat, DBC_{total}: total double bond conversion, $t_{95\%}$: time to reach 95% of DBC_{total}.

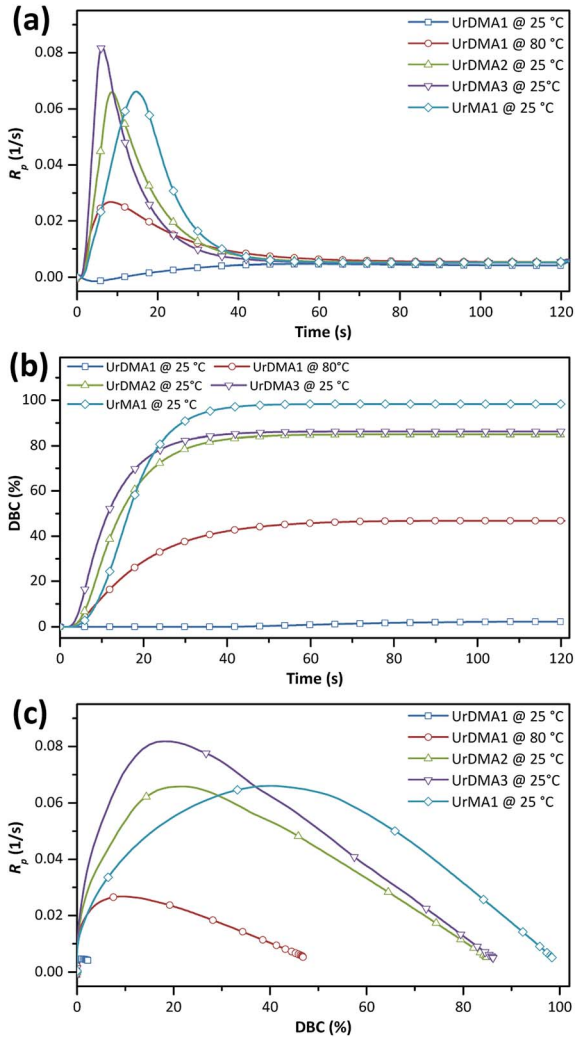

Fig. 3 Photo-curing rate (a and c) and double bond conversion (b) for urethane-methacrylates obtained from photo-DSC data.

TPO-L. The photo-curing rate (R_p) and double bond conversion (DBC) values as a function of time were calculated from photo-DSC data (Fig. S5 in ESI†) and presented in Fig. 3 and Table 1. UrDMA1 containing TPO-L, which was solid at room temperature showed very low photo-reactivity (DBC_{total} = 2%) at 25 °C. Therefore, photo-DSC was repeated for this sample at a higher temperature (80 °C). All samples exhibited the auto-acceleration and auto-deceleration phenomenon, *i.e.* an initial increase and a later decrease in R_p, respectively (Fig. 3a), as well as a maximum limiting conversion during the photo-curing process (Fig. 3b). This complex behavior is because the mobility of the methacrylate groups gradually decreases over the photo-curing time. Initially, the R_p of liquid monomers, an overall of the propagation and termination rates, is constant and chemical-controlled. Later, due to an increase in the viscosity of the photo-curing mixture the coupling of macroradicals for the termination is diffusion-limited, while the monomers are still mobile for the propagation, thus R_p increases (auto-acceleration). Finally, the reaction mixture is transformed from a liquid to a rubbery or glassy network, which significantly restricts the diffusion of monomers to reach the macroradicals, therefore R_p decreases (auto-deceleration). Due to the gelation or vitrification, all methacrylate groups can not react and the final conversion is less than unity.[11]

UrDMA1 cured even at 80 °C showed a lower photo-reactivity ($R_{p,max} = 2.68 \times 10^{-2}$ s^{-1}) and conversion (DBC_{total} = 47%) comparing to UrDMA2 ($R_{p,max} = 6.59 \times 10^{-2}$ s^{-1}, DBC_{total} = 85%). Although UrDMA1 molecules have higher potency to pre-associate *via* intermolecular hydrogen bonding comparing to the amorph UrDMA2 molecules, the reaction of methacrylate groups within this high viscosity melted mixture (at 80 °C) was diffusion-limited. The photo-reactivity of the synthesized UrDMA1 was lower than the reported values ($R_{p,max} = 9 \times 10^{-2}$ s^{-1}, DBC_{total} = 78% (ref. 7)), which can be related to the differences in the purity of monomer and experiment parameters. UrDMA3 with the balanced intermolecular hydrogen bonding (UrDMA1 > UrDMA3 > UrDMA2) and viscosity (UrDMA1 > UrDMA3 > UrDMA2) displayed the highest photo-reactivity (t_{max} = 10.9 s, $R_{p,max} = 8.18 \times 10^{-3}$ s^{-1}) and conversion (DBC_{total} = 86%) compared to UrDMA1 and UrDMA3. Higher conversion of UrDMA3 is also related to the higher molecular flexibility of the corresponding photo-curing mixture (UrDMA3 > UrDMA2 > UrDMA1)[11] arising from two flexible ether bonds within its molecular structure. Plotting R_p *versus* DBC presented interesting facts (Fig. 3c). Reaching high DBC_{total} values is important since the mechanical strength of the urethane-methacrylates is dependent on their conversion during photo-curing.[12] UrDMA1 with higher viscosity and lower molecular flexibility reached $R_{p,max}$ at lower conversion (9.2%), while $R_{p,max}$ for UrDMA2 and UrDMA3 observed at higher conversions (21.3% and 18.0%, respectively) due to lower viscosity and higher molecular flexibility of the corresponding photo-curing mixtures.

Monofunctional UrMA1 showed a slower photo-curing (t_{max} = 19.5 s) but higher conversion (DBC_{total} = 98%) comparing to the difunctional urethane-methacrylates. Due to the monofunctionality, the viscosity of the photo-curing mixture did not increase sharply leading to a delayed gelation point, where the whole methacrylate groups remained mobile and active until the end of the polymerization. Due to the same reason, UrMA1 reached $R_{p,max}$ at much higher conversion (40.3%).

Thermal, physical, and mechanical properties of cured samples

Mixtures of each monomer and TPO-L (3 wt%) were poured into Teflon or silicone molds (depth of 0.5 mm) and cured with a UV lamp under an Ar atmosphere. All the cured samples were denoted with a prefix "X" following the name of the corresponding monomer. The thermal transitions of the cured sample were determined using DSC. The first and second heating cycles were used for the extraction of T_g values (middle point of base-line change, Table 2 and Fig. S6 in ESI†). For all difunctional urethane-methacrylates, the T_g values of the cured samples were significantly increased in the second heating cycle comparing to the first cycle, probably due to the thermally-

Table 2 Thermal and viscoelastic properties of cured samples[a]

	DSC		DMA					
	T_g (°C)							
Sample	1st cycle	2nd cycle	T_g (°C)	tan δ_{max}	$E'_{25\,°C}$ (MPa)	$E'_{rubbery}$ (MPa)	$T_{rubbery}$ (K)	ν_c (mol m^{-3})
XUrDMA1	50	100	126	0.41	2100	24	140	2360
XUrDMA2	45	81	85	0.32	1720	105	127	10 550
XUrDMA3	45	57	80	0.40	1670	49	108	5140
XUrMA1	25	24	51	1.50	1070	20	55	2500

[a] tan δ_{max}: loss coefficient (loss modulus/storage modulus) at T_g, $E'_{25\,°C}$: storage modulus at 25 °C, $E'_{rubbery}$: storage modulus in the rubbery region, T: the absolute temperature at the beginning of the rubbery plateau.

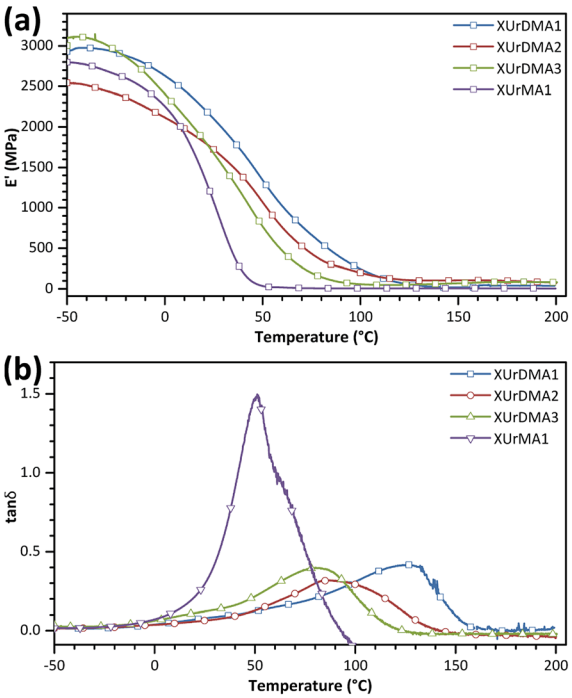

Fig. 4 Storage modules and tan δ curves for cured samples.

initiated polymerization of the unreacted methacrylate groups within the samples at elevated temperatures (120–200 °C). The T_g values for the cured samples were also determined *via* DMA (peak of the tan δ curve, Fig. 4 and Table 2). As expected, the T_g values obtained from DMA were higher than the values determined by DSC, due to differences in the analysis principles and parameters,[41,42] but represented the same trend. XUrDMA3 showed the lowest T_g values compared to XUrDMA1 and XUrDMA2 due to the existence of flexible ether bonds within its structure, which can confirm the high flexibility for the photo-curing UrDMA3 mixture as a reason for its high conversion. Meanwhile, XUrDMA2 had lower T_g values than XUrDMA1 due to the sterical hindrance effect of two methyl groups increasing the free volume between the crosslinked urethane-methacrylate backbones.

The XUrMA1 supposed to be a thermoplastic displayed an exothermic melting peak at 188 °C ($\Delta H_m = 3.6$ J g^{-1}). Due to the mono-functionality of UrMA1, *i.e.* less possibility for chemical crosslinking, XUrMA1 showed lower T_g values and a higher loss coefficient (tan $\delta_{max} = 1.50$) comparing to other cured samples based on the difunctional monomers (Fig. 4b). Due to the complete conversion of the methacrylate group of UrMA1 during the photo-curing process ($DBC_{total} = 98\%$), the T_g value obtained from DSC for XUrMA1 did not change in the second heating cycle compared to the first cycle (Fig. S6 in ESI†).

The viscoelastic data obtained from DMA (Fig. 4a and Table 2) showed higher storage modulus (E') at room temperature for XUrDMA1 ($E'_{25\,°C} = 2100$ MPa) compared to XUrDMA2 ($E'_{25\,°C} = 1720$ MPa) and XUrDMA3 ($E'_{25\,°C} = 1670$ MPa), which is attributed to the higher ability of its urethane-methacrylate backbone for hydrogen bonding resulting in the physical crosslinking. In contract, at the elevated temperatures (beginning of the rubbery, 108–140 °C), where no hydrogen

Table 3 Physical properties and thermal stability of cured samples[a]

			TGA		
Sample	Gel content (%)	Water absorption (%) in PBS after 7 d	$T_{5\%}$ (°C)	$T_{50\%}$ (°C)	$T_{90\%}$ (°C)
XUrDMA1	100 ± 1	4 ± 1	290	429	479
XUrDMA2	99 ± 1	4 ± 1	212	402	472
XUrDMA3	99 ± 1	4 ± 1	217	405	451
XUrMA1	89 ± 4	2 ± 1	215	357	436

[a] $T_{5\%}$: temperature with weight loss of 5%, $T_{50\%}$: temperature with weight loss of 50%, $T_{90\%}$: temperature with weight loss of 90%.

bonding occurs, XUrDMA1 displayed a lower E' value ($E'_{\text{rubbery}} = 24$ MPa) compared to XUrDMA2 ($E'_{\text{rubbery}} = 105$ MPa) and XUrDMA3 ($E'_{\text{rubbery}} = 49$ MPa), which can be related to the lower content of crosslinking points within its structure. Therefore, the crosslink density (ν_c, mole number of network chains per unit volume) for all cured samples was calculated based on DMA data.[43] As expected, XUrDMA1 had the lowest ν_c value (2360 mol m^{-3}) due to the low conversion of methacrylate groups (47%). The higher ν_c value for XUrDMA2 (10 550 mol m^{-3}) compared to XUrDMA3 (5140 mol m^{-3}), with the similar DBC_{total} values, can be explained based on the lower molecular weight of its urethane-methacrylate backbone (457 g mol^{-1} *versus* 517 g mol^{-1}).

The gel content of the cured samples was determined through extraction with acetone (Table 3). A conversion of 47% during the photo-curing UrDMA1 was enough to provide a gel content of 100% for XUrDMA1, similar to XUrDMA2 and XUrDMA3. Surprisingly, XUrMA1 based on the monofunctional monomer exposed a gel content of 89%, which can be attributed to the backbiting effect, *i.e.* radical abstraction of tertiary hydrogens for butyl moiety,[44,45] during the photo-curing process, which led to partial crosslinking of the poly(urethane-methacrylate) chains. Checking the gel content of XUrMA1 using more polar solvents, *i.e.* THF and DMSO, resulted in the same values. It is worth to mention that the XUrMA1 sample was unstable in acetone and broken into small pieces, which demonstrated the low level of chemical crosslinking within its structure.

The bulk hydrophilicity of the cured samples was evaluated by measuring the water absorption in phosphate-buffered saline (PBS, pH = 7.4) at 37 °C (Table 3 and Fig. S7 in ESI†). All cured samples showed a water absorption of less than 4% in PBS. XUrMA1 displayed a lower water absorption (2%) comparing to other cured samples based on the difunctional monomers (4%), which can be attributed to the higher hydrophobicity of its urethane-methacrylate backbone as well as the presence of crystalline domains resisting against the penetration of water molecules inside the samples. The presence of hydrophilic ether bonds within the XUrDMA3 backbone facilitated the absorption of water molecules, reaching 4% in 1 d (Fig. S7 in ESI†), but did not increase the overall equilibrium water absorption after 7 d compared to XUrDMA1 (Table 3). It is worth to mention that the absorbed water molecules could effectively plasticize the urethane-methacrylate backbone of the cured samples. For example, the hard and brittle XUrDMA1 sample turned flexible after immersing in PBS (Fig. 5).

Fig. 5 Pictures for XUrDMA1 before (left) and after (right) immersion in PBS.

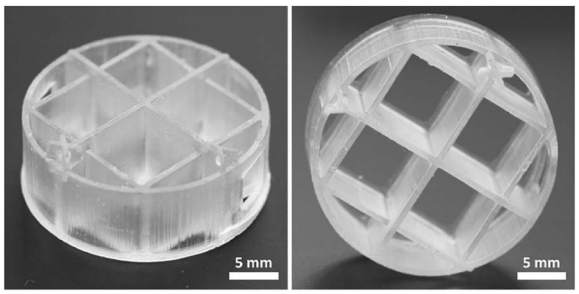

Fig. 6 Pictures for 3D printed test object using an ink based on the monomers.

The thermal stability of the cured samples was evaluated by TGA (Table 3 and Fig. S8 in ESI†). Results revealed that all samples were thermally stable at least up to 212 °C ($T_{5\%}$, the temperature at which 5% weight loss took place) under an N_2 atmosphere. The cured samples underwent a two-step thermal degradation (Fig. S8 in ESI†) starting with a weight loss at 210–350 °C regarding the thermal degradation of urethane bonds.[34,43] Urethane bonds are known to be relatively thermally unstable generating primary amine/olefin or secondary amine/carbon dioxide upon degradation.[34,43] The second weight loss at 350–480 °C is attributed to the degradation of their uncrosslinked/crosslinked aliphatic backbones.[34,43,46] Surprisingly, XUrDMA1 with lower DBC_{total} and ν_c values exposed higher thermal stability ($T_{5\%} = 290$ °C) than XUrDMA2 ($T_{5\%} = 212$ °C) and XUrDMA3 ($T_{5\%} = 217$ °C). One explanation could be the thermally-initiated polymerization of the unreacted methacrylate groups within samples at elevated temperatures, which is in agreement with the increasing of T_g values in the second heating cycle of DSC (Table 2 and Fig. S6 in ESI†). As expected, XUrMA1 with a partially crosslinked structure demonstrated a weight loss profile at lower temperatures compared to other cured samples based on the difunctional monomers (Fig. S8 in ESI†).

3D printing of urethane-methacrylates

The 3D printability of the monomers was evaluated on a commercial DLP printer operating at 365 nm. For this purpose, a mixture of monomers containing TPO-L was used as an ink (the formulation is not reported). The ink was very reactive and successfully 3D printed to a complex object with a curing time of 3 s for one layer of 100 μm (Fig. 6). After 3D printing, the objects were washed thoroughly with isopropanol to remove the unreacted ink and post-cured with a UV lamp. The printed objects displayed high accuracy and precision as the designed model (Fig. S9 in ESI†).

Conclusions

Urethane-methacrylate monomers were synthesized *via* a safe and environmentally friendly route without using any toxic

isocyanates or tin-based catalysts. The chemical structure of the urethane block was effective on the photo-reactivity (R_p and DBC_{total}) of the monomers and the physicomechanical properties of the cured samples. The incorporation of side methyl groups or ether bonds within the urethane block can be employed to change the intermolecular hydrogen bonding for improving the photo-reactivity of the monomer as well as the flexibility and crosslinking density of the cured samples. An ink was developed based on the monomers and successfully 3D printed using a DLP machine. Through the non-isocyanate route, a wide range of starting materials, *i.e.* amines and cyclic carbonates, can be used to synthesis new urethane-methacrylates with desirable photo-reactivity and physicomechanical properties for the 3D printed samples. We are now using these monomers for 3D printing of flexible biomedical materials, which will be published in the future.

Conflicts of interest

There are no conflicts to declare.

Acknowledgements

The authors acknowledge the financial support by the Federal Ministry of Education and Research of Germany in the framework of "ProMatLeben – Polymere" (project number 13XP5087E, PolyKARD).

References

1 J. W. Hong, H. K. Cheon, S. H. Kim, K. H. Hwang and H. K. Kim, *Prog. Org. Coat.*, 2017, **110**, 122–127.
2 M. Wrosch, G. Xian and V. M. Karbhari, *J. Appl. Polym. Sci.*, 2008, **107**, 3654–3662.
3 M. Yin, F. Liu and J. He, *J. Mech. Behav. Biomed. Mater.*, 2016, **57**, 157–163.
4 J. Seo, D. I. Kushner and M. A. Hickner, *ACS Appl. Mater. Interfaces*, 2016, **8**, 16656–16663.
5 D. K. Patel, A. H. Sakhaei, M. Layani, B. Zhang, Q. Ge and S. Magdassi, *Adv. Mater.*, 2017, **29**, 1606000.
6 J. F. G. A. Jansen, A. A. Dias, M. Dorschu and B. Coussens, *Macromolecules*, 2003, **36**, 3861–3873.
7 H. J. Assumption and L. J. Mathias, *Polymer*, 2003, **44**, 5131–5136.
8 T. Y. Lee, T. M. Roper, E. S. Jönsson, C. A. Guymon and C. E. Hoyle, *Macromolecules*, 2004, **37**, 3659–3665.
9 M. T. Lemon, M. S. Jones and J. W. Stansbury, *J. Biomed. Mater. Res., Part A*, 2007, **83**, 734–746.
10 I. M. Barszczewska-Rybarek, *Dent. Mater.*, 2009, **25**, 1082–1089.
11 I. Sideridou, V. Tserki and G. Papanastasiou, *Biomaterials*, 2002, **23**, 1819–1829.
12 I. Barszczewska-Rybarek, *Polym. Bull.*, 2017, **74**, 4023–4040.
13 *MDI and TDI: a safety, health and the environment: a source book and practical guide*, ed. D. C. Allport, D. S. Gilbert and S. M. Outterside, J. Wiley, New York, 2003.
14 C. A. Redlich, D. Bello and A. V. Wisnewski, in *Environmental and occupational medicine*, Lippincott Williams & Wilkins, Philadelphia, 4th edn, 2007, pp. 502–516.
15 J. E. Lockey, C. A. Redlich, R. Streicher, A. Pfahles-Hutchens, P. Bert, J. Hakkinen, G. L. Ellison, P. Harber, M. Utell, J. Holland, A. Comai and M. White, *J. Occup. Environ. Med.*, 2015, **57**, 44–51.
16 C. A. Redlich and M. H. Karol, *Int. Immunopharmacol.*, 2002, **2**, 213–224.
17 S. Gagné, J. Lesage, C. Ostiguy and H. Van Tra, *Analyst*, 2003, **128**, 1447–1451.
18 C. A. Krone, J. T. A. Ely, T. Klingner and R. J. Rando, *Bull. Environ. Contam. Toxicol.*, 2003, **70**, 328–335.
19 C. A. Krone and T. D. Klingner, *Pediatr. Allergy Immunol.*, 2005, **16**, 368–379.
20 D. Bello, C. A. Herrick, T. J. Smith, S. R. Woskie, R. P. Streicher, M. R. Cullen, Y. Liu and C. A. Redlich, *Environ. Health Perspect.*, 2007, **115**, 328–335.
21 M. C. Tanzi, P. Verderio, M. G. Lampugnani, M. Resnati, E. Dejana and E. Sturani, *J. Mater. Sci.: Mater. Med.*, 1994, **5**, 393–396.
22 M. Nath, *Appl. Organomet. Chem.*, 2008, **22**, 598–612.
23 L. Meng, X. Wang, M. Ocepek and M. D. Soucek, *Polymer*, 2017, **109**, 146–159.
24 L. Meng, M. D. Soucek, Z. Li and T. Miyoshi, *Polymer*, 2017, **119**, 83–97.
25 Y. Deng, S. Li, J. Zhao, Z. Zhang, J. Zhang and W. Yang, *RSC Adv.*, 2014, **4**, 43406–43414.
26 S. Li, J. Zhao, Z. Zhang, J. Zhang and W. Yang, *RSC Adv.*, 2015, **5**, 6843–6852.
27 M. S. Kathalewar, P. B. Joshi, A. S. Sabnis and V. C. Malshe, *RSC Adv.*, 2013, **3**, 4110.
28 X. Wang and M. D. Soucek, *Prog. Org. Coat.*, 2013, **76**, 1057–1067.
29 M. Decostanzi, C. Bonneaud and S. Caillol, *J. Polym. Sci., Part A: Polym. Chem.*, 2019, **57**, 1224–1232.
30 H. Quan, T. Zhang, H. Xu, S. Luo, J. Nie and X. Zhu, *Bioact. Mater.*, 2020, **5**, 110–115.
31 Q. Yan, H. Dong, J. Su, J. Han, B. Song, Q. Wei and Y. Shi, *Engineering*, 2018, **4**, 729–742.
32 J. J. Warner, P. Wang, W. M. Mellor, H. H. Hwang, J. H. Park, S.-H. Pyo and S. Chen, *Polym. Chem.*, 2019, **10**, 4665–4674.
33 G. Rokicki and A. Piotrowska, *Polymer*, 2002, **43**, 2927–2935.
34 H. Bakhshi, H. Yeganeh, S. Mehdipour-Ataei, A. Solouk and S. Irani, *Macromolecules*, 2013, **46**, 7777–7788.
35 H. Bakhshi and S. Agarwal, *Polym. Chem.*, 2016, **7**, 5322–5330.
36 M. Blain, L. Jean-Gérard, R. Auvergne, D. Benazet, S. Caillol and B. Andrioletti, *Green Chem.*, 2014, **16**, 4286–4291.
37 H. Tomita, F. Sanda and T. Endo, *J. Polym. Sci., Part A: Polym. Chem.*, 2001, **39**, 3678–3685.
38 R. M. Garipov, V. A. Sysoev, V. V. Mikheev, A. I. Zagidullin, R. Ya. Deberdeev, V. I. Irzhak and Al. Al. Berlin, *Dokl. Phys. Chem.*, 2003, **393**, 289–292.
39 F. Camara, S. Benyahya, V. Besse, G. Boutevin, R. Auvergne, B. Boutevin and S. Caillol, *Eur. Polym. J.*, 2014, **55**, 17–26.

40 C. Li, S. Li, J. Zhao, Z. Zhang, J. Zhang and W. Yang, *J. Polym. Res.*, 2014, **21**, 498.
41 S. Kasapis, I. M. Al-Marhoobi and J. R. Mitchell, *Carbohydr. Res.*, 2003, **338**, 787–794.
42 C. A. Gracia-Fernández, S. Gómez-Barreiro, J. López-Beceiro, J. Tarrío Saavedra, S. Naya and R. Artiaga, *Polym. Test.*, 2010, **29**, 1002–1006.
43 H. Bakhshi, H. Yeganeh, A. Yari and S. K. Nezhad, *J. Mater. Sci.*, 2014, **49**, 5365–5377.
44 H. Bakhshi, H. Bouhendi, M. J. Zohuriaan-Mehr and K. Kabiri, *J. Appl. Polym. Sci.*, 2010, **117**, 2771–2780.
45 H. Bakhshi, M. J. Zohuriaan-Mehr, H. Bouhendi and K. Kabiri, *J. Mater. Sci.*, 2011, **46**, 2771–2777.
46 H. Bakhshi and S. Agarwal, *J. Mater. Chem. B*, 2017, **5**, 6827–6834.